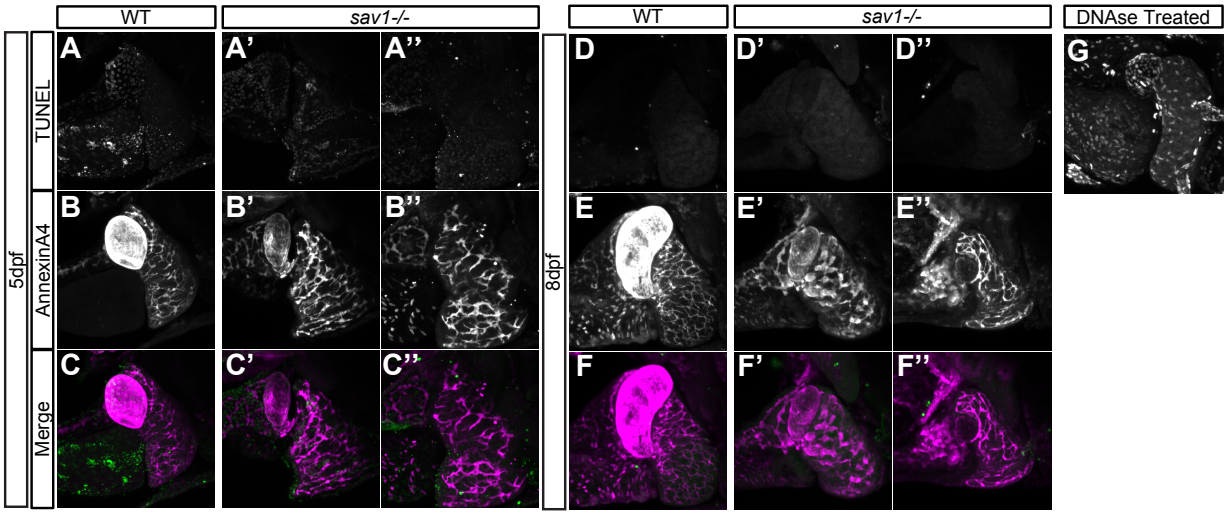

Figure S1. Abnormal biliary duct morphology, and loss of AnnexinA4 in gallbladder of *sav1-/-* larvae is not associated with biliary cell death. (A-A'') TUNEL staining of WT and *sav1-/-* larvae at 5dpf. There is no significant detection of TUNEL labeling at this time point in either WT or *sav1-/-* larvae regardless of phenotype severity. (B-B'') AnnexinA4 labeling in WT and *sav1-/-* fish to indicate phenotype severity. (C-C'') Merged images of A-A'' and B-B'' with AnnexinA4 stain in magenta, and TUNEL stain in green. *n=6* WT; *n=8 sav1-/-*. (D-F'') These panels depict TUNEL and AnnexinA4 whole-mount staining following the same labeling convention as A-C'' but at 8dpf. *n=4* WT; *n=11 sav1-/-*. (G) WT larvae at 8dpf treated with DNAse for 15 min serves as a positive control for TUNEL detection.

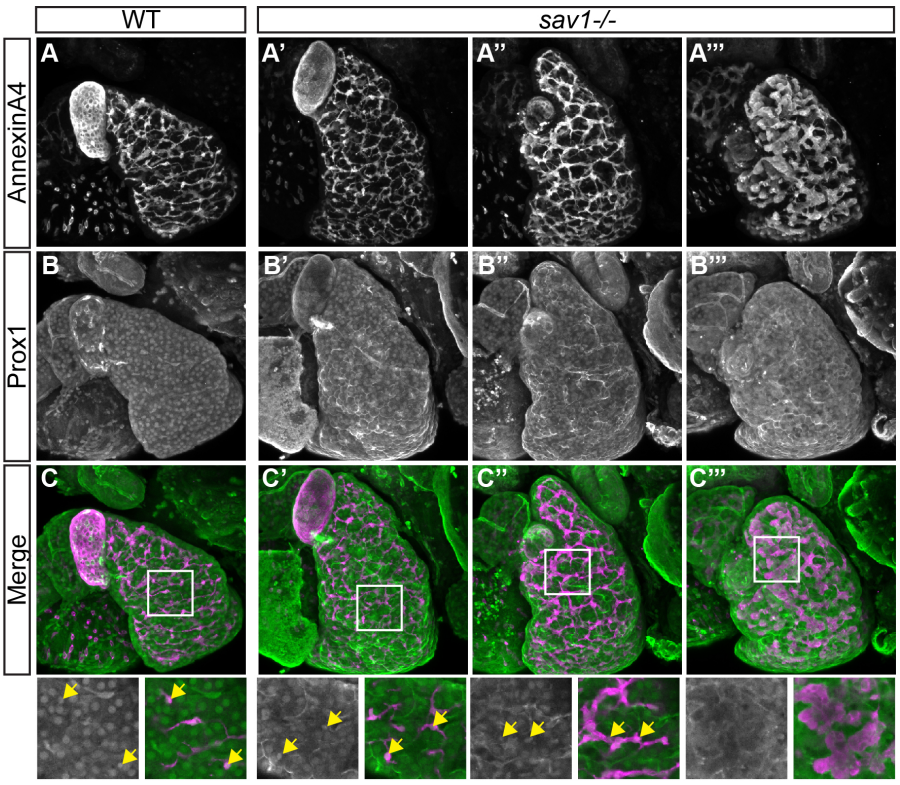

Figure S2. *sav1-/-* mutants lose Prox1 immunostaining in biliary cells with abnormal morphology. (A-A’’’) Whole-mount staining for AnnexinA4 in WT and *sav1-/-* larvae at 8dpf. (B-B’’’) Whole-mount staining of the same larvae from A-A’’’ for Prox1. (C-C’’’) Merged images of A-A’’’ and B-B’’’ with AnnexinA4 stain in magenta, and Prox1 stain in green. Single plane enlarged images corresponding to the white boxes shown in C-C’’’ are found below each merged image, with the left image showing grayscale Prox1 staining, and the right image depicting the merged image. Yellow arrows point to nuclear localized Prox1 labeling of intrahepatic biliary epithelial cells. Prox1 labels nuclei of both hepatocytes and biliary epithelial cells at 8dpf in WT and *sav1-/-* mutants characterized as normal or mild. Biliary epithelia in mutants with moderate or severe phenotypes lose Prox1 labeling. *n=4* WT; *n=7 sav1-/-*.

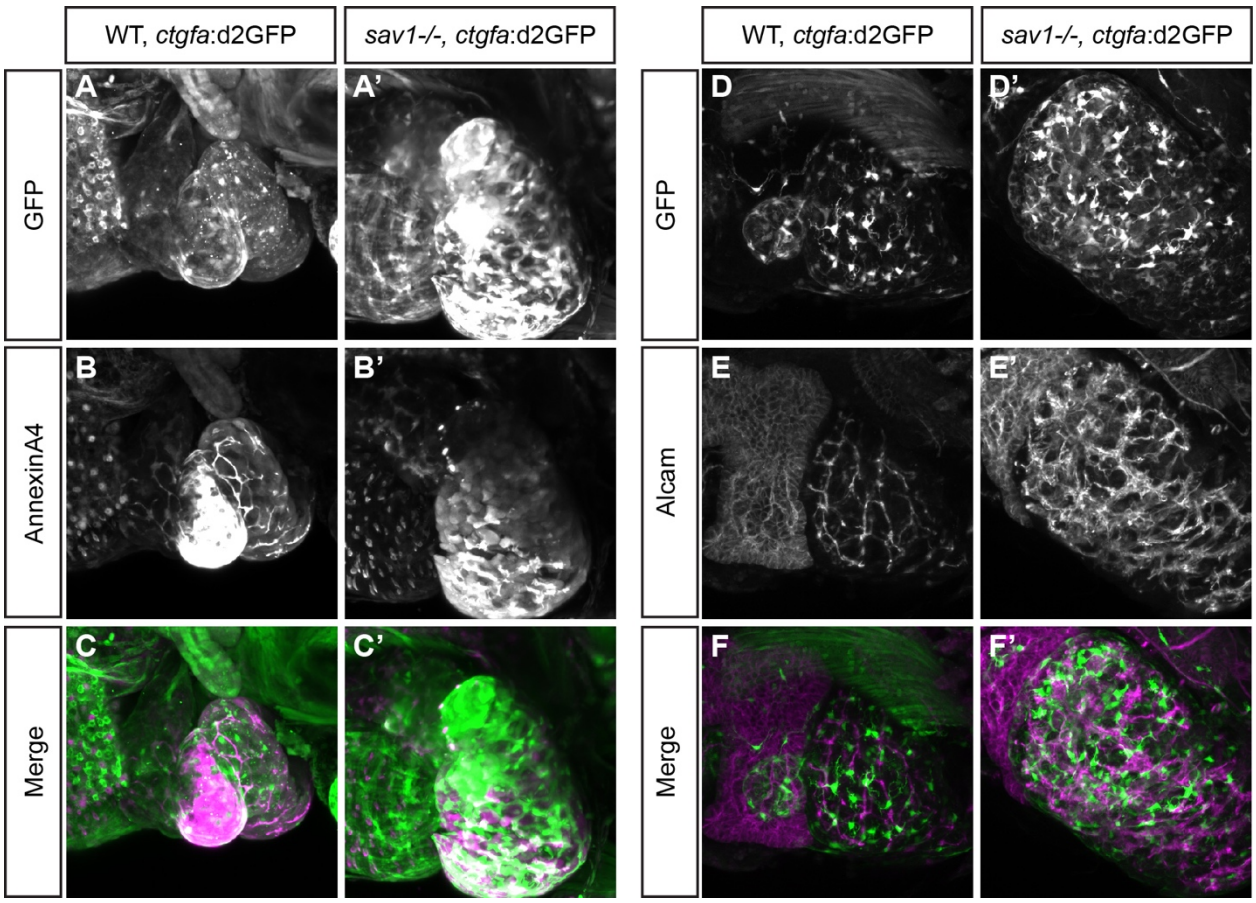

Figure S3. The Yap/Taz reporter *ctgfa*:d2GFP is elevated in both biliary cells and nonbiliary cells with deletion of *sav1*. (A-A', D-D') GFP staining of WT and *sav1-/-* larvae at 7dpf. WT fish show expression in gallbladder and sporadic cells located throughout the liver. (B-B') AnnexinA4 staining of WT and *sav1-/-* larvae at 8dpf. (C-C') Merged images of A-A' and B-B' with AnnexinA4 in magenta, and GFP in green. *n=5* WT; *n=4 sav1-/-*. Merged images show that in WT larvae *ctgfa*:d2GFP+ cells within the liver are often distinct from the intrahepatic biliary network with their morphology resembling hepatic stellate cells. In *sav1-/-* mutants, the fluorescent intensity and number of these cells are increased. *ctgfa*:d2GFP also is more highly expressed in *sav1-/-* mutant AnnexinA4+ cells with abnormal morphology. (E-E') Alcam staining of WT and *sav1-/-* larvae at 8dpf. (F-F') Merged images of A-A' and B-B' with AnnexinA4 in magenta, and GFP in green. *n=5,* WT; *n=6, sav1-/-*. Merged images show the majority of *ctgfa*:d2GFP+ cells in WT larvae are distinct from Alcam outlined biliary network.

Again in *sav1-/-* mutants, *ctgfa*:d2GFP expression is present in these nonbiliary cells as well as in Alcam+ cells with abnormal morphology.

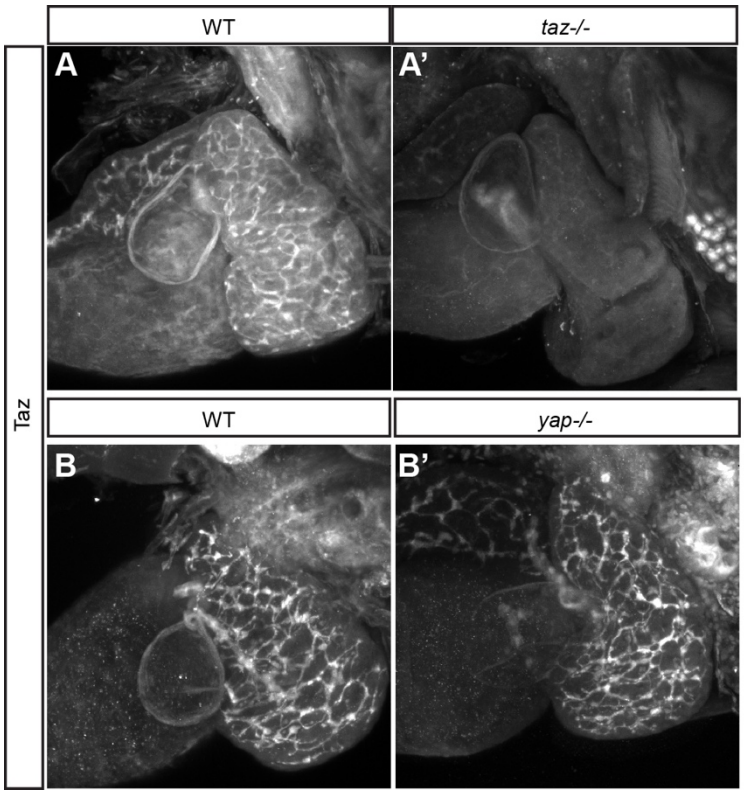

Figure S4. The Yap/Taz Cell Signaling antibody D24E4 selectively labels Taz within the biliary system. (A,B) Yap/Taz Cell signaling antibody D24E4 whole-mount staining in WT 8dpf larvae. Staining labels the entire biliary system. (A') Staining of *taz-/-* larvae with this antibody results in the loss of this signal. *n=9* WT, *n=4 taz-/-*, (B') Staining of *yap-/-* larvae with this antibody is indistinguishable from WT siblings. *n=6* WT *n=3 yap-/-*.

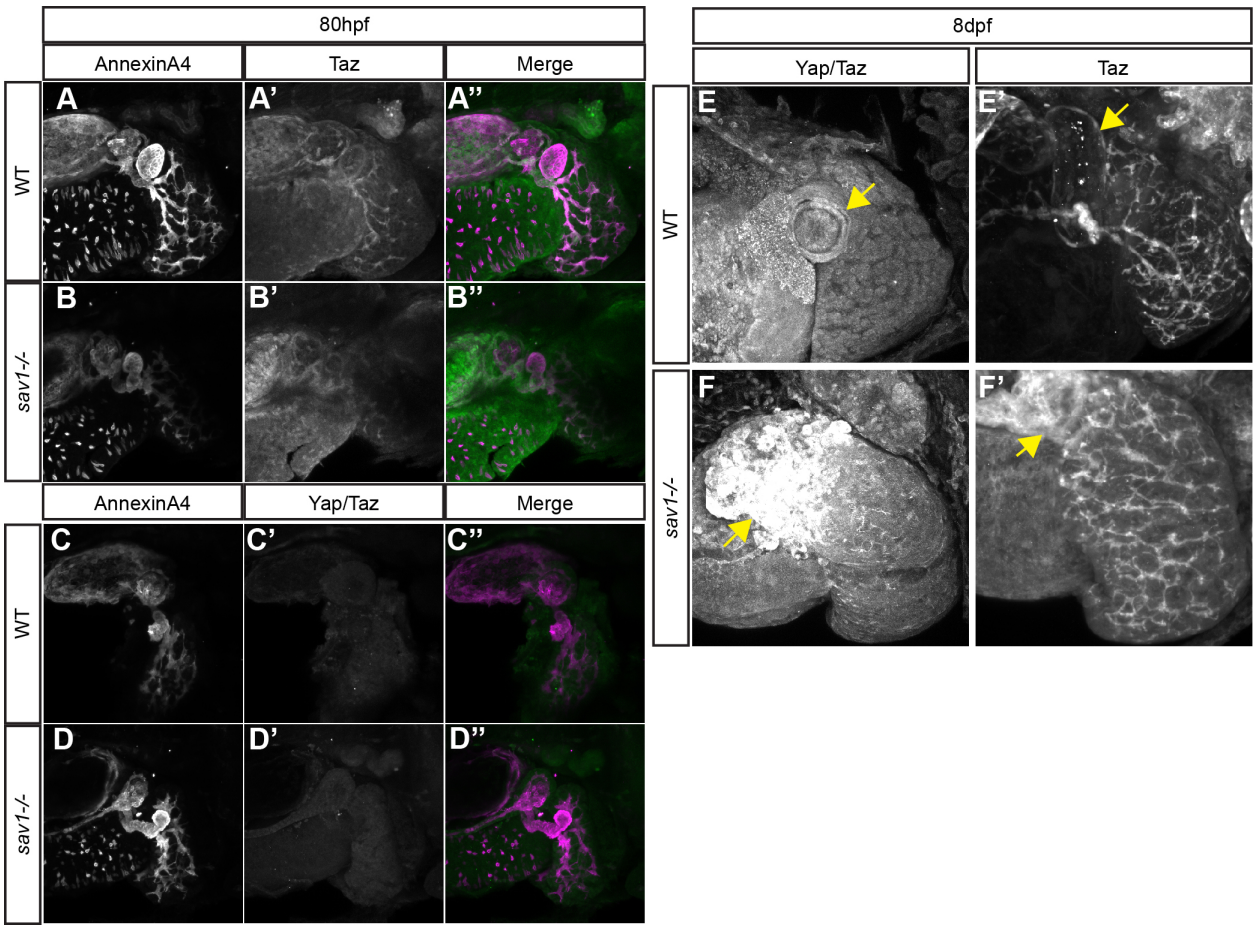

Figure S5. Comparison of Yap/Taz staining and Taz staining in WT and *sav1-/-* larvae. (A-B'') Taz and AnnexinA4 double staining at 80hpf reveal that Taz is enriched in the WT biliary system and unaltered in *sav1-/-* mutants, *n=3* WT; *n=3 sav1-/-.* (C-D'') In contrast Yap/Taz and AnnexinA4 double staining at 80hpf reveals low levels of staining in liver and pancreas without enrichment in the biliary system. Yap/Taz staining is similar between WT larvae and *sav1-/-* mutants, *n=4* WT; *n=5 sav1-/-* (E) Yap/Taz whole-mount staining at 8dpf of WT larvae shows consistent levels of staining throughout liver and gallbladder. *n=6* WT (E') In contrast, Taz whole-mount staining at 8dpf is restricted to the biliary system. *n=15* WT (F) Yap/Taz staining of *sav1-/-* larvae shows increase fluorescent intensity, particularly in the normal anatomic location of the gallbladder. *n=9 sav1-/-.* (F') Taz staining of *sav1-/-* larvae also shows similar increases in fluorescent intensity at this position while retaining expression throughout the biliary system. *n=13 sav1-/-.* Yellow arrows indicate gallbladders in WT fish (A-A'), and the normal position of the gallbladder in *sav1-/-* siblings (B-B').

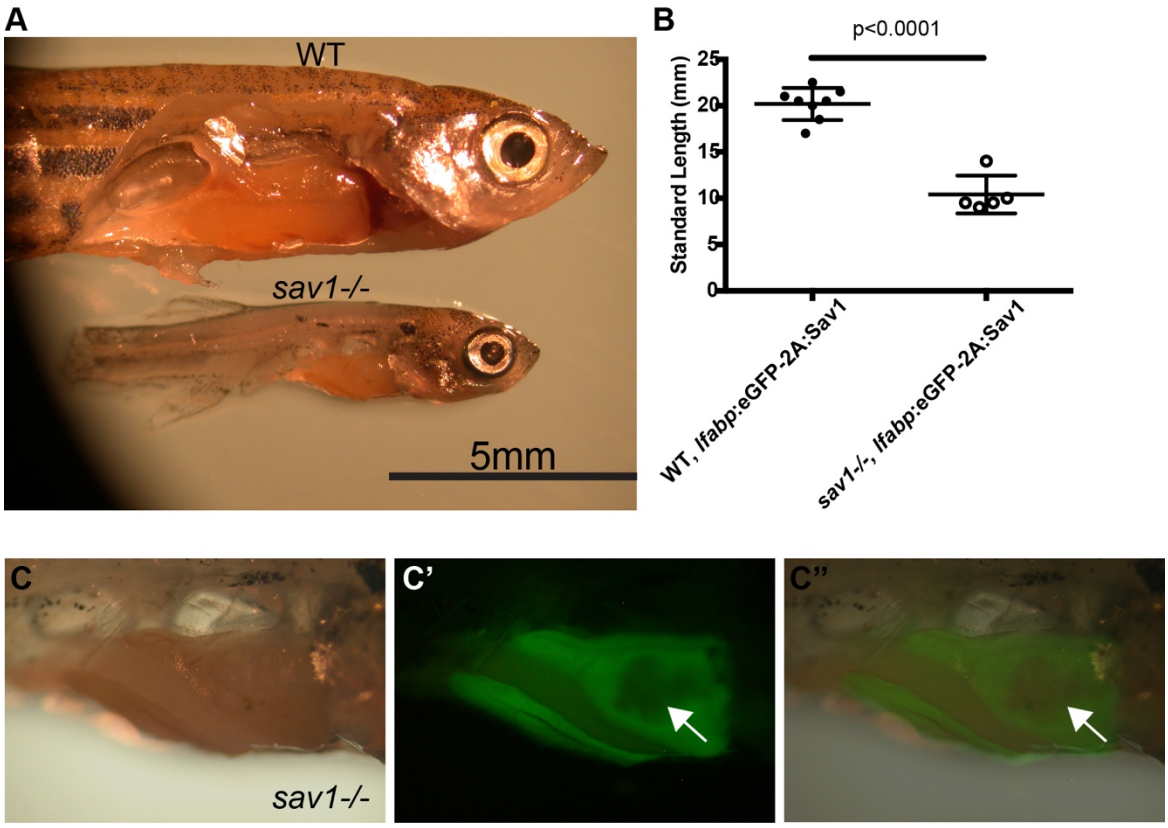

Figure S6. *sav1-/-*;*lfabp*:eGFP-2a:Sav1 fish are smaller than WT *lfabp*:eGFP-2a:Sav1 siblings and display regions of liver dysplasia. (A) Micrographs of WT and *sav1-/-* age-matched siblings transgenic for *lfabp*:eGFP-2a:Sav1 demonstrate the differences in size. (B) Quantification of (A). Standard length of zebrafish in millimeter (mm) shows that *sav1-/-;lfabp*:eGFP-2a:Sav1 fish are significantly smaller than their WT;*lfabp*:eGFP-2a:Sav1 siblings. *n=8* WT; *n=5 sav1-/-*. (C-C'') Brightfield and GFP fluorescent images of *sav1-/-;lfabp*:eGFP-2a:Sav1 liver, showing the loss of fluorescence present at the normal anatomical position of the gallbladder.

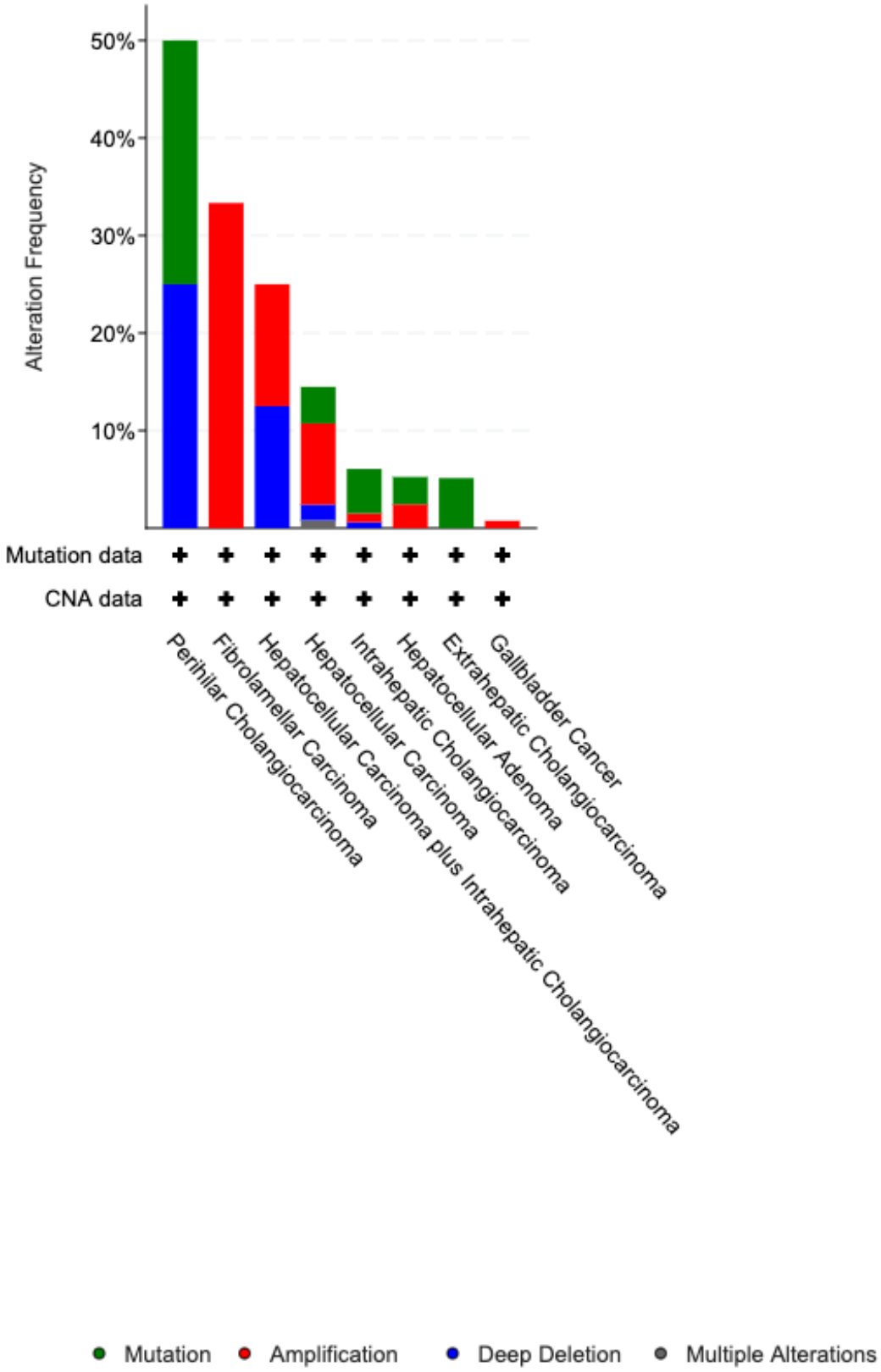

Figure S7. Genes for core Hippo pathway components are altered in biliary tract carcinomas. Data curated by cBioPortal from 15 studies on liver or biliary tract cancers were queried for alterations in the following core Hippo pathway components: SAV1, STK3, STK4, LATS1, LATS2, MOB1A, MOB1B, YAP1, and WWTR1. 151 of 1657 patient samples (~9%) had alterations in these Hippo pathway components. Furthermore, while the number of samples available for extrahepatic biliary tract cancers is relatively small compared to liver cancers generally, alterations in several Hippo pathway components are present. While only 4 samples of perihilar cholangiocarcinoma were available, 2 of these had alterations in the pathway, with 1 containing a deep deletion in SAV1, and the other a mutation in STK3. 39 cases were identified as extrahepatic cholangiocarcinoma, and 2 of these samples had mutations in YAP1. Finally, 1 out of 134 cases of gallbladder carcinomas were altered, identifying a LATS1 amplification. Y-axis represents the percentage of samples within the X-axis group that had alterations in at least one of the genes queried. CNA; copy number amplification.

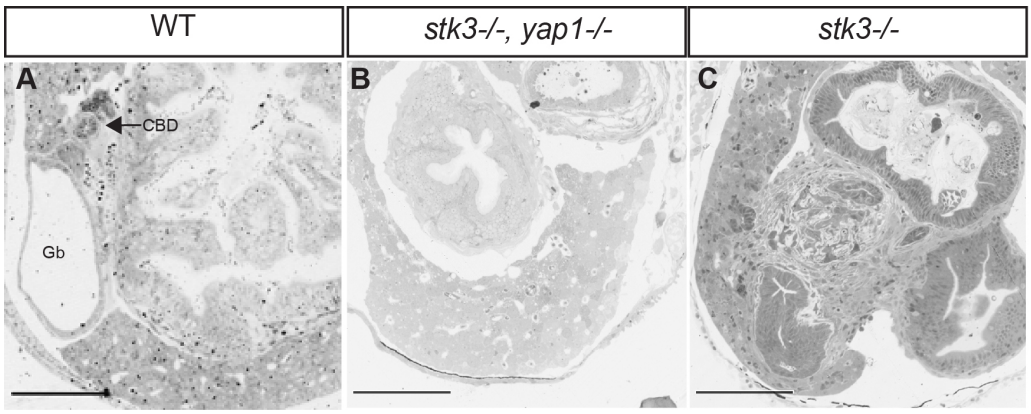

Figure S8. Loss of *yap* rescues abnormal biliary morphology in *stk3-/-* fish. (A-C) Toluidine Blue stained plastic sections of liver and gallbladder in WT, *stk3*-/-, and *stk3*-/-;*yap*-/- larvae at 16dpf, revealing rescue of gallbladder and common bile duct morphology. *n=5* WT; *n=3 stk3-/-*; *n=2 stk3-/-;yap-/-*. Gb; gallbladder, CBD; common bile duct.

	Perihilar Cholangiocarcinoma		Fibrolamellar Cholangiocarcinoma	Hepatocellular Carcinoma plus Intrahepatic Cholangiocarcinoma		Hepatocellular Carcinoma				Intrahepatic Cholangiocarcinoma			Hepatocellular Adenoma		Extrahepatic Cholangiocarcinoma	Gallbladder Carcinoma
	Mutation	Deep Deletion	Amplification	Amplification	Deep Deletion	Mutation	Amplification	Deep Deletion	Multiple Alterations	Mutation	Amplification	Deep Deletion	Mutation	Amplification	Mutation	Amplification
SAV1		1			1	1	2	3		3		2				
STK3	1		1	1		5	50	1	2		4		2	6		
STK4						2	1			1						
LATS1						13	1	8		2			2			1
LATS2						7	2	1		5			4	1		
MOB1A						1				1			1			
MOB1B							1									
YAP1						5	2	1		2					2	
WWTR1						3	10			1						
TOTAL ALTERATIONS	1	1	1	1	1	37	67	15	2	15	4	2	9	7	2	1
TOTAL CASES WITH ALTERATIONS	2		1	2		108				20			15		2	1
TOTAL CASES	4		3	8		746				330			286		39	134
ALTERATION FREQUENCY	50%		33.333%	25%		14.48%				6.606%			5.24%		5.13%	0.75%

Table S1. Genetic alterations to Hippo pathway components in biliary and liver carcinomas. Annotated summary of cBioPortal data of liver cancer subtypes associated with genetic alterations in Hippo pathway components.